AJRCMB Articles in Press. Published on 02-February-2018 as 10.1165/rcmb.2017-0413OC

# TRPV4-stimulation releases ATP via pannexin channels in human pulmonary fibroblasts

*Mozibur Rahman[§], Rui Sun[§], Subhendu Mukherjee[§], Bernd Nilius[*] and Luke J. Janssen[§]*

§ Firestone Institute for Respiratory Health, St. Joseph's Hospital, Department of Medicine, McMaster University, Hamilton, Ontario, Canada L8N 3Z5

* KU Leuven, Department of Cellular and Molecular Medicine, Laboratory of Ion Channel Research, B-3000 Leuven, Belgium

**Running title:** Pannexin channels and currents in human pulmonary fibroblasts

[†]**Correspondence**: Dr. Luke Janssen

St. Joseph's Hospital, 50 Charlton Ave. East, L-314

Hamilton L8N 4A6, Ontario, Canada.

phone: 1-905-522-1155

Fax: 1-905-540-6510

Email: janssenl@mcmaster.ca

**Source(s) of support**: Canadian Institutes of Health Research

**Author contributions**: LJJ designed the study, interpreted the data and drafted the manuscript. MR performed electrophysiological experiments and analyzed those data. SM and RS collaborated in performing the confocal fluorimetry and Western blots and analyzing those data. BN provided expertise with respect to TRP channel physiology and assisted in interpretation of the data. All authors contributed to refinement of the submitted manuscript. LJJ takes overall guarantee for the paper.

**Impact statement**: Ionic currents play a key role in a wide variety of cellular functions, and yet very little is known about fibroblast electrophysiology. In this paper, we explore a cascade of ionic conductances (TRPV4, pannexin and ATP-ligand-gated channels) which lead to elevation of [Ca2+] and ATP-release. Other studies have implicated these conductances in fibrotic changes.

AJRCMB Articles in Press. Published on 02-February-2018 as 10.1165/rcmb.2017-0413OC

**Abstract**

We previously described several ionic conductances in human pulmonary fibroblasts (HPFs), including one activated by two structurally distinct TRPV4-channel agonists: 4α-phorbol-12,13-didecanoate (4αPDD) and GSK1016790A. However, the TRPV4-activated current exhibited peculiar properties: it developed slowly over many minutes, exhibited reversal potentials that could vary by tens of millivolts even within a given cell, and was not easily reversed by subsequent addition of two distinct TRPV4-selective blockers (RN-1734 or HC-067047). In this study, we characterized that conductance more carefully. We show here that 4αPDD stimulated a delayed release of ATP into the extracellular space which was reduced by genetic silencing of pannexin expression, and that the 4αPDD-evoked current could be blocked by apyrase (rapidly degrades ATP) or by the P2Y purinergic receptor-channel blocker PPADS, and could be mimicked by exogenous addition of ATP. We further show the 4αPDD-evoked current to be blocked by pre-treating with RN-1734 or HC-067047, by $Gd^{3+}$ or $La^{3+}$, or by two distinct blockers of pannexin channels (carbenoxolone or probenecid), but not by a blocker of connexin hemi-channels (flufenamic acid). We also found expression of TRPV4- and pannexin channel proteins. 4αPDD markedly increased calcium-flashing in our cells, the latter was abrogated by the P2Y channel blocker PPADS, and the 4αPDD-evoked current was eliminated by loading the cytosol with BAPTA or by inhibiting $Ca^{2+}$/calmodulin-sensitive kinase II (CamK-II) using KN93. Altogether, we interpret these findings to suggest that 4αPDD triggers ATP-release via pannexin channels, which in turn acts in an autocrine and/or paracrine fashion to stimulate PPADS-sensitive purinergic receptors on HPFs.

**Key words:** fibroblasts; pulmonary fibrosis; TRPV4; pannexin-1; electrophysiology

**Conflict of Interest:** None of the authors have any conflict of interest pertaining to this work.

AJRCMB Articles in Press. Published on 02-February-2018 as 10.1165/rcmb.2017-0413OC

## Introduction

Idiopathic pulmonary fibrosis (IPF) is a devastating lung disease with a daunting prognosis. In the past, very little could be done to help IPF patients, outside of lung transplantation, until the recent introduction of nintedanib and pirfenidone [1] [2] [3], but even these pharmacological interventions are only partially effective, and their mechanisms of action are still very poorly understood. New avenues of therapy for IPF are much needed.

Lung fibroblasts are responsible for the fibrosis seen in IPF. Though their biology has been reasonably well studied, one area which has been particularly overlooked is their electrophysiology [4]. Certain ion channels may play a role in lung diseases such as IPF. For example, the expression of two groups of genes is markedly increased in IPF patients, among which the "most significant cluster of genes that are upregulated" include TRPV4-channels (transient receptor potential, vanilloid-type, subtype 4) [5]. The latter have been implicated in bleomycin-induced pulmonary fibrosis [6]. TRPV4 channels are often functionally coupled to various proteins, including pannexin-channels [7] [8], which are large conductance pores that conduct a wide variety of ions and water-soluble molecules less than ~1000 Da, including ATP [9] [10] [11] [12]. TRPV4 activation leads to ATP release in the lung [7] as it does in many other cell types [13] [14] [15], and we have previously shown that stimulation of lung fibroblasts with ATP leads to increased expression of matrix proteins and alpha smooth muscle actin (indicating transformation to a myofibroblast phenotype) through ATP-gated P2Y receptor/channels [16].

We have recently described [17] a very large membrane conductance in human pulmonary fibroblasts stimulated with 4α-phorbol-12,13-didecanoate (4αPDD) or GSK1016790A, both of which activate TRPV4-channels [18] [11] [19] [20] [21] (although

4αPDD can also act through other pathways [22] [23]. We were puzzled, however, to find that this putative TRPV4-current developed very slowly, exhibited a widely varying reversal potential (+/-20 mV) which drifted substantially within any given cell, and was not easily reversed by highly TRPV4-selective antagonists such as RN-1734 [24] or HC-067047 [18]. The inhibitory effect of those antagonists was augmented, however, when combined with chloride channel blockers such as di-isothiocyano-2,2'-stilbenedisulfonic acid (DIDS) or niflumic acid [17]. The strange electrophysiological properties of this 4αPDD-evoked conductance may be a consequence of the coupled opening of TRPV4-channels and pannexin-channels, leading to release of ATP and additional opening of ATP-gated receptor/channels. A recent report described pannexin-mediated release of ATP in subcutaneous fibroblasts following bradykinin-induced $Ca^{2+}$-signaling, leading to autocrine stimulation via $P2Y_{12}$ receptors [25]. We therefore sought within this study to explore the interactions between these three distinct conductances in human pulmonary fibroblasts.

Pannexins are a relatively novel group of channel-forming glycoproteins which comprises three family members. Pannexin 1 (Panx1) is ubiquitously expressed in many mammalian tissues, while Panx2 and Panx3 may be less widely expressed [26] [12]. Panx1 exhibits exceptionally large unitary conductance (~500 pS; [9] [11]) and is activated by a variety of stimuli, including strong depolarization, mechanical stress, elevation of intracellular [$Ca^{2+}$], cleavage of its C-terminal by caspase 3/7, nitrosylation and phosphorylation [27] [28] [11] [9] [10] [29] [30]. Some studies suggest it is involved in recruitment of phagocytes toward apoptotic cells via paracrine signaling (release of ATP) [31] [26]. Several pharmacological tools have been employed in studies of pannexin channel physiology. Carbenoxolone (CBX; a synthetic derivative of the licorice-derived β-stereoisomer of 18-glycyrrhetinic acid) [32] and probenecid

AJRCMB Articles in Press. Published on 02-February-2018 as 10.1165/rcmb.2017-0413OC

(an organic anion transport inhibitor) [28] exhibit much greater selectivity against pannexin-currents than against connexin-currents (a very closely related conductance), while the chloride channel blockers flufenamic acid [32] or 5-nitro-2(3-phenylpropylamino)-benzoic acid (NPPB) [28] exhibit the reverse selectivity. Pannexin currents can also be suppressed by other chloride channel blockers such as niflumic acid [27], and by non-selective cation channel blockers such as the trivalent ions gadolinium ($Gd^{3+}$) and lanthanum ($La^{3+}$) [27].

These new revelations of pannexin- and TRPV4-channel physiology, pharmacology and interactions now raised a new possibility in our minds. Here, we hypothesize that TPRV4-channels in human pulmonary fibroblasts couple with pannexin channels, leading to the release of endogenous ATP, which in turn acts on purinergic receptor/channel complexes in an autocrine fashion. This cascade of events explains the paradoxical findings we have reported previously [17].

## Methods

### Isolation and Culture of Fibroblasts

All experimental procedures were approved by the St Joseph's Hospital Board of Ethics. HPFs were obtained from the lungs of six patients (three male and three female; aged 60–80 yr) undergoing lung surgery for pulmonary nodules following informed consent. None of the patients had major respiratory co-morbidities or lung function abnormalities. Normal lung tissues were taken from macroscopically-normal lung areas, as distant from the nodules as possible, and passaged repeatedly (only passages 4-10 were used in experiments).

### Electrophysiology

Whole-cell patch-clamp electrophysiology was performed on freshly trypsinized cells. To block $K^+$-currents and shift the Cl- equilibrium potential to -50 mV, we substituted KCl in the electrode solution with 120 mM $Cs^+$-aspartate plus 20 mM CsCl, as described previously [17]; 50 μM β–escin was included to effect permeabilization of the membrane patch.

Current-voltage relationships were quickly assessed using ramp depolarizations (parameters as indicated in the text), delivered at 15 second intervals.

### Confocal calcium fluorimetry

Intracellular [$Ca^{2+}$] was monitored in confluent cells using Oregon Green and a custom-built apparatus, as we have described previously [16] [17] [33] [34] [35] . Images were acquired at 3 second intervals before and during application of 10 μM 4αPDD (10 μM).

### ATP-assay

AJRCMB Articles in Press. Published on 02-February-2018 as 10.1165/rcmb.2017-0413OC

Cells were cultured in 96-well plates for 2 days, then challenged with 4αPDD (5 μM) for varying periods of time, after which the supernatant overlying these cells was aspirated and assayed (in duplicate) at various times for ATP-content using a commercially-available bioluminescent ATP assay (Sigma Aldrich) at room temperature. In a follow-up assay, cells were pre-treated with silencing-RNA against pannexin channels, or a scrambled si-RNA probe.

**Western blots**

Western blot analysis was done as described previously [16] using antibodies raised against TRPV4 or against Panx1 (Abcam , Toronto, ON, Canada) and whose immuno-specificities have been verified elsewhere [36] [37].

**siRNA transfection**

Cells were transfected using control siRNA (Qiagen) or pannexin 1 siRNA (Thermo Fisher Scientific), then used in patch-clamp, confocal fluorimetric and ATP-assay studies 48 hours later.

**RNA isolation and RT-PCR**

Total RNA was isolated, treated with DNAse, reverse transcribed, amplified, and visualized as described previously [29]. using qScript™ cDNA SuperMix (Quanta Bioscience, Gaithersburg, MD, USA).

**Data Analysis**

Membrane currents were standardized by expressing as a fraction of the total cell capacitance.

Calcium-flash frequency was expressed as the number of flashes seen during the 200 frames immediately before addition of 4αPDD, as well as the 200 frames following addition of that agent. In those cells in which we subsequently tested the effect of PPADS, we compared the number of flashes during 200 frames of 4αPDD alone versus the number during 4αPDD plus PPADS.

Data are presented as means ± SEM and significant differences were detected using the Student's *t* test or one-way ANOVA, as indicated ($p < 0.05$). *n* indicates the numbers of isolated cells tested.

AJRCMB Articles in Press. Published on 02-February-2018 as 10.1165/rcmb.2017-0413OC

## Results

### 4αPDD acts through stimulation of ATP-release

HPFs held under voltage-clamp and stimulated with 4αPDD (5 μM) exhibited a time-dependent increase in membrane current (Fig. 1) with an ohmic I-V relationship (Fig. 2A) and a reversal potential ($V_{rev}$) which ranged as much as 20 mV above and below 0 mV in no particular direction (Fig. 2D): we have described this response previously [17], and the reader is directed there for representative examples with full current–voltage (I–V) relationships showing the shift in $V_{rev}$ within any given cell. Generally speaking, relatively little current was evident during the first few minutes after application of 4αPDD, but this grew substantially in magnitude without seeming sometimes to reach a maximum even after 20-30 minutes. The growth of this current in several representative cells is shown in Fig. 1A (inset displays a portion of the same data on an expanded vertical axis), while the mean magnitudes of this current at 5 minute intervals in all cells tested are given in Fig. 1B. As we have shown previously, $V_{rev}$ for this 4αPDD-evoked current would shift markedly during the course of the 20-30 minutes in which it evolved. This is exemplified within Fig. 2D (far left), in which the small diamonds indicate the full range of reversal potentials seen within a given cell, while the large squares indicate the mean (+/- standard deviation) of those two ranges.

Previously [17], we were puzzled at our finding that this electrophysiological response to a TRPV4-selective agonist was not easily reversed by subsequent application of the TRPV4-selective blockers RN-1734 or HC-067047. A mechanism whereby 4αPDD acts through release of some other autacoid might explain the slow development of this current and the lack of inhibition when TRPV4-selective blockers were applied after the fact. We here examined whether those same TRPV4-selective blockers were more effective when applied prior to

4αPDD (by suppressing the entire cascade). We did indeed find that such pretreatment largely reduced the development of the 4αPDD-evoked membrane current, but still did not abolish it Fig. 1).

In order to determine whether 4αPDD works indirectly through a purinergic signaling pathway, we next investigated the effect of PPADS (10 μM) upon the 4αPDD-evoked current; elsewhere, we have shown that particular blocker of P2Y receptors [38] to be effective in blocking the actions of exogenously-added ATP in HPFs [16]. Pre-application of PPADS greatly reduced the 4αPDD-evoked membrane current (Fig. 1). The I-V relationship of the residual current remaining after this PPADS-pretreatment was also ohmic with a mean $V_{rev}$ of approximately -5 mV (Fig. 2D); interestingly, we noted very little variability over time in $V_{rev}$ during PPADS-treatment (Fig. 2D).

We also examined the effect of apyrase, which degrades extracellular ATP by catalyzing its breakdown to ADP. We found the electrophysiological response to 4αPDD (5 μM) was also significantly reduced by pretreating the cells for 10 minutes with this ectonucleotidase (10 units) prior to stimulation with 4αPDD (Figure 1 and 2A), and that the variability in $V_{rev}$ was again greatly reduced (Fig. 2D).

Next, we examined the electrophysiological response in these cells to exogenously-added ATP ($10^{-5}$ M in application pipette, applied at a distance of ~100 microns from the cell; the final concentration experienced at the cell surface cannot be determined, but would of necessity be substantially lower than this concentration and may vary during the application due to incomplete mixing). ATP also evoked a large ohmic current (Fig. 2B); this developed gradually over the course of many minutes (Fig. 2C, bottom trace). As was the case for the 4αPDD-evoked current, $V_{rev}$ within any given cell tended to drift dramatically over the course of 20-25 minutes

AJRCMB Articles in Press. Published on 02-February-2018 as 10.1165/rcmb.2017-0413OC

(Fig. 2C, top trace). On average, the $V_{rev}$ for the ATP-evoked current was also ~ 0 mV, albeit with a very wide range of values (Fig. 2D). This current was immediately abolished by subsequent application of $Gd^{3+}$ (1 mM; Figure 2B); in 8 cells tested in this way, the ATP-evoked current measured at -80 mV was significantly reduced from -47.3±9.5 pA/pF to -6.0±2.8 pA/pF by $Gd^{3+}$.

Finally, to demonstrate directly that 4αPDD stimulates HPFs to release ATP, we performed a luciferase assay to detect the accumulation of ATP in the media of HPFs stimulated with 4αPDD (5 μM). For the first 15 minutes, ATP levels did not rise above the detection limit of the assay; however, at 20 minutes there was a substantial accumulation of ATP in the bathing medium surrounding the cells, and some further increase by 30 minutes (Figure 3). In cells pretreated with apyrase, there was no accumulation of ATP when measured at 30 minutes (Fig. 3).

Altogether, these findings suggest strongly that 4αPDD acts by triggering the release of ATP, which in turn acts in an autocrine and/or paracrine fashion to stimulate PPADS-sensitive purinergic receptors on these cells [38].

$Gd^{3+}$ has been shown to block TPRV4-channels (but activate other TRP-channels) [8] [23] [18] [39], as well as Panx1- [11], purinergic- [38], and volume-regulated chloride-channels [40] [41] [42] [43] [44]. Consistent with this, we found $Gd^{3+}$ (1 mM) completely blocked all 4αPDD-evoked current in these cells. Despite the non-specificity of this agent, its abrupt inhibitory action here is revealing in that it shows this slowly developing current is not simply an artefact of cell death or degradation of the giga-ohm seal.

Likewise, $La^{3+}$ blocks many TRP-channels, including TRPV4, but augments others [8] [18] [45] [46]. At -80mV, cells pretreated with $La^{3+}$ evolved a conductance of 0.3±1.6pA/pF.

This grew to 2.8±1.8 pA/pF upon addition of 4αPDD, which is significantly smaller than the control 4αPDD-evoked response.

**4αPDD activates PanX1 channels**

To ascertain whether pannexin channels were involved in the release of intracellular ATP, we compared the effects of pretreating the cells with agents which act against pannexins and/or connexins prior to stimulating with 4αPDD. We found the Panx1-selective blockers CBX or probenecid markedly reduced the magnitude of the 4αPDD–evoked current (Fig. 1) and greatly reduced the range of $V_{rev}$ derived from the currents which remained following such treatment (Fig. 2D). However, the connexin-selective blocker flufenamic acid (100 μM) was much less effective in reducing the magnitude of the 4αPDD–evoked current (Fig. 1A and 1B) and did not reduce the variability in $V_{rev}$ (Fig. 2D).

Western blots confirmed the presence of TRPV4 channel and pannexin channel proteins in our cells (Fig. 4A). Likewise, PCR showed the presence of pannexin channel transcripts which could be eliminated using silencing RNA constructs targeted against PANX1, but which were unaffected by a scrambled siRNA control construct (Fig. 4B). More importantly, cells which had been pretreated with PANX1-specific silencing RNA exhibited little or no membrane current response to 4αPDD, whereas other cells pretreated with the scrambled control RNA exhibited substantial 4αPDD-evoked currents (Fig. 4C).

**Coupling of the TRPV4-channels to PanX-channels**

Panx1 channels can be activated by elevations of cytosolic [$Ca^{2+}$] (see Discussion). We hypothesized that activation of TRPV4-channels by 4αPDD led to influx of external $Ca^{2+}$ and

AJRCMB Articles in Press. Published on 02-February-2018 as 10.1165/rcmb.2017-0413OC

accumulation in the cytosol to levels which activate Panx1 channels. To test this possibility, we pre-loaded the cells with BAPTA-AM for 50 minutes prior to stimulating with 4αPDD (5 μM): this pre-treatment greatly reduced the mean magnitude of the 4αPDD-evoked current (Fig. 1) and the variability in $V_{rev}$ (Fig. 2D).

Others [47] have shown a Panx1-mediated response in tumor cells which is sensitive to the $Ca^{2+}$/calmodulin-dependent protein kinase II (CamKII) inhibitor KN93. We also tested the effect of that inhibitor (10 μM) on the response described in our preparation, finding it also inhibited the 4αPDD-evoked membrane current in HPFs (Fig. 1).

**Confocal imaging of intracellular $Ca^{2+}$**

We have previously shown that exogenously-applied ATP, applied by direct pressure-ejection from a micropipette brought into proximity of the cell, evokes a spike-like $Ca^{2+}$-transient, sometimes accompanied by recurring $Ca^{2+}$-spikes, in HPFs [16]. Here we examined whether 4αPDD also evokes $Ca^{2+}$-spikes, and whether they could be modulated by inhibiting P2Y receptors using PPADS. We did indeed find that 4αPDD (5 μM), applied by addition to the media superfusing the cells, markedly increased the rate of firing of $Ca^{2+}$-spikes (Fig. 5A), and that this firing rate was abruptly suppressed by PPADS (10 μM; Fig. 5B).

## Discussion

In our previously published electrophysiological characterization of the basal ionic conductances present in HPFs, we reported a very large ohmic conductance which was activated by two structurally different agents which activate TRPV4-channels (4αPDD and GSK1016790A) [17]. However, several features of this current were puzzling.

First, it developed very slowly, building over the course of many minutes even though agonists and antagonists of other currents acted within seconds, indicating the problem was not due to delayed delivery of the drug to the cells.

Second, the reversal potential for these agonist-evoked currents could differ by 10-20 mV between cells, and could also drift by another 10-20 mV within any given cell (for example, see Fig. 2D, the reversal potentials for 4αPDD alone). In contrast, we did not see this degree of variability in determinations of voltages of activation or inactivation in another type of ionic conductance, the "L-type" voltage-dependent $Ca^{2+}$-channel, indicating this variability in the reversal potential of the TRPV4-associated current was not due to electrode drift, poor grounding, or inadequate voltage clamp.

Third, the agonist-evoked currents were not easily reversed after the fact (i.e., once they had developed) by two highly TRPV4-selective antagonists: RN-1734 or HC-067047.

Our interpretation of the data obtained in this present study now explain these three paradoxical observations. Our data suggest that stimulation of the TRPV4 channels leads to opening of pannexin channels and release of ATP, which in turn acts in an autocrine fashion on purinergic ion channel/receptors which we have described previously (see Figure 6) [16]. Others have described a similar pathway operating in other cell types, including sensory nerves of guinea-pigs [48].

AJRCMB Articles in Press. Published on 02-February-2018 as 10.1165/rcmb.2017-0413OC

Although ATP can also permeate calcium homeostasis modulator 1 (CALHM1) and its *Caenorhabditis elegans* homolog, CLHM-1, we do not believe the latter are involved in this phenomenon because those channels are insensitive to CBX or probenecid [49].

In our previous study of ATP-evoked $Ca^{2+}$-spike activity [16], we found the fluorimetric response to ATP to be nearly instantaneous (relative to the long delay in electrophysiological response to 4αPDD seen in the present study). That relatively long delay in build-up of this TRPV4-agonist-evoked current could be due to the relatively slow accumulation of ATP in the extracellular space, and/or to the various signaling events which must occur within the cells, such as the stimulation of CamKII and phosphorylation of its target(s). Likewise, we did not find that $Ca^{2+}$-spike activity in any given cell led to $Ca^{2+}$-spikes in immediately adjacent cells, presumably because ATP did not accumulate to sufficient levels before it was swept away within the perfused experimental chamber.

The wide shifts in $V_{rev}$ of the TRPV4-evoked current is explained by the fact that at least three distinct conductances — TRPV4-, pannexin- and P2Y-channels — are ultimately and concurrently activated by the TRPV4-agonists. All three are mixed cationic conductances (the relative permeability of different cations may vary between them) with $V_{rev}$ in the vicinity of 0 mV. Furthermore, our previous study [17] suggests that a chloride conductance may also be activated by 4αPDD (the complexity of the electrophysiological repertoire of these cells has stymied our investigation of this possibility), and pannexin-channels can also conduct chloride; the equilibrium potential for chloride in the present study is -50 mV. Altogether, then, the varying changes over time in the cationic and anionic conductances in these cells produced by the sequential activation of TRPV4-, pannexin- and P2Y-channels can explain the wide ranges in Vrev we noted previously [17] and in the present study. Another explanation for drift in $V_{rev}$ may

be changes in the electrochemical gradients across the HPF membranes for the permeant ions as these various conductances become activated and those gradients become dissipated.

The lack of efficacy of the TRPV4-selective blockers against the 4αPDD- or GSK1016790A-evoked currents, when applied after the latter had already developed, may reflect the fact that those blockers would not impact the pannexin- or ATP-mediated currents which would also be active following stimulation with 4αPDD or GSK1016790A. We also showed in our previous study that supplementing the application of TRPV4-selective blockers with the chloride channel blocker DIDS was more effective, and interpreted that as possibly indicating the involvement of chloride currents. We now add another interpretation: that the chloride channel blocker was actually blocking the pannexin channels, as several other chloride channel blockers have been shown to do.

Several have shown Panx1 is activated by a wide variety of stimuli which exert numerous diverse actions, but which all share in common their ability to stimulate influx of extracellular $Ca^{2+}$: these include excitotoxic NMDA channels [9]; ionotropic purinergic P2X receptors [10] [12]; strong membrane depolarization [50] [11] [12] [10] which can activate voltage-dependent $Ca^{2+}$-channels; stretch [12] with consequent activation of mechanosensitive ion channels; and stimulation of several G-protein-coupled receptors [10]. Conflicting observations make it unclear whether this is due to elevation of cytosolic [$Ca^{2+}$] per se [11], or instead is due to a transient depletion of extracellular $Ca^{2+}$ around the mouth of the Panx1 channels following massive $Ca^{2+}$-influx [10] [11]. During the course of this study and our previous one, we found that the delivery of many dozen strongly depolarizing voltage commands alone eventually induced some ohmic current which complicated analysis of the effects of various blockers. This is not due to a progressive deterioration of the seal between the membrane and the electrode nor

AJRCMB Articles in Press. Published on 02-February-2018 as 10.1165/rcmb.2017-0413OC

the prolonged invasive nature of our electrophysiologic experiment (these recordings involve more than 20 minutes of dialysis at the end of an electrode during repeated strong depolarizations) nor induction of apoptosis or necrosis, since it was immediately abolished by $Gd^{3+}$ (we intentionally used this poorly selective blocker in order to abrogate a wide variety of conductances and thereby establish that the current was an electrophysiological event and not a technical artefact). Moreover, the cells did not appear blebbed, phase-dark, or translucent. We believe that the progressive development of this ohmic membrane current during prolonged experiments using repeated ramp commands represents a delayed and progressive activation of Panx1 current in response to the strongly depolarizing pulses themselves. Furthermore, we speculate that this is due to elevation of cytosolic $[Ca^{2+}]$ since it was nearly abolished by pretreatment with BAPTA. The depolarizations may open L-type $Ca^{2+}$-channels which we have characterized previously [17], while 4αPDD can also trigger influx through TRPV4-channels.

$Ca^{2+}$ may open the pannexin channels directly [11], or may act by stimulating CamK-II activity, since we also found the TRPV4-evoked current to be sensitive to the CamK-II inhibitor KN93. Alternatively, elevation of $[Ca^{2+}]$ may stimulate some other enzymatic activity, including a kinase (Panx1 is phosphorylated by Src family kinases [9]) or a $Ca^{2+}$-dependent protease (which might cleave the C-terminal, as caspase 3/7 is known to do [27] [28] [11] [10] [9] [29] [30]. We did not investigate these many diverse possibilities in this study.

The physiological role played by pannexin channels in HPFs is still unclear. They may account for certain mechanosensitive functions of these cells, since mechanosensation is accompanied by ATP-release. Others have shown a role for TRPV4 and pannexin-channels in cigarette smoke-induced ATP release in the lung, as well as increased expression of TRPV4 in lung tissue samples from patients with COPD [7]. Similarly, our group [34] and another [6] have

described the involvement of these ionic mechanisms in bleomycin-induced pulmonary fibrosis. Yang et al. found mRNA expression to be markedly altered in patients with idiopathic pulmonary fibrosis and usual interstitial pneumonia (IPF/UIP) compared to non-diseased controls [5]. In particular, they were able to divide the IPF/UIP patients into two groups, the one disease group showing marked up-regulation of two distinct gene clusters (comprised of 80 and 51 genes, respectively) and down-regulation of a third cluster, associated with greater microscopic honeycombing (but not fibroblastic loci) relative to the other diseased group. More importantly, the "most significant cluster of genes that are upregulated" included TRPV4 and calmodulin.

In conclusion, these findings suggest that 4αPDD acts by triggering the release of ATP, which in turn acts in an autocrine and/or paracrine fashion to stimulate PPADS-sensitive purinergic receptors on HPFs. This mechanism of action, involving the concurrent activation of TRPV4-, pannexin- and P2Y-conductances would account for the slow development of the 4αPDD-evoked current, its relative insensitivity to TRPV4-blockers once the current has developed, and our finding that $V_{rev}$ can vary by tens of millivolts. This complex electrophysiological response may be important in lung pathologies such as COPD and lung fibrosis.

AJRCMB Articles in Press. Published on 02-February-2018 as 10.1165/rcmb.2017-0413OC

**Acknowledgements**

Funding was provided by the Canadian Institutes for Health Research. The authors wish to acknowledge Dr. Martin Kolb and Fuqin Duan for kindly providing us with HPFs.

## REFERENCES

[1] W. Wuyts, M. Kolb, S. Stowasser, W. Stansen, J. Huggins and G. Raghu, "First Data on Efficacy and Safety of Nintedanib in Patients with Idiopathic Pulmonary Fibrosis and Forced Vital Capacity of </=50 % of Predicted Value," *Lung,* vol. 194, pp. 739-743, 2016.

[2] G. Hughes, H. Toellner, H. Morris, C. Leonard and N. Chaudhuri, "Real World Experiences: Pirfenidone and Nintedanib are Effective and Well Tolerated Treatments for Idiopathic Pulmonary Fibrosis," *J. Clin. Med,* vol. 5, pp. 5-9, 2016.

[3] C. Albera, U. Costabel, E. Fagan, M. Glassberg, E. Gorina, L. Lancaster, D. Lederer, S. Nathan, D. Spirig and J. Swigris, "Efficacy of pirfenidone in patients with idiopathic pulmonary fibrosis with more preserved lung function," *Eur. Respir. J.,* vol. 48, pp. 843-851, 2016.

[4] L. Janssen, S. Mukherjee and K. Ask, "Calcium-homeostasis and Ionic Mechanisms in Pulmonary Fibroblasts," *Am. J. Respir. Cell Mol. Biol.,* vol. 53, pp. 135-148, 2015.

[5] I. Yang, C. Coldren, S. Leach, M. Seibold, E. Murphy, J. Lin, R. Rosen, A. Neidermyer, D. McKean, S. Groshong, C. Cool, G. Cosgrove, D. Lynch, K. Brown, M. Schwarz, T. Fingerlin and D. Schwartz, "Expression of cilium-associated genes defines novel molecular subtypes of idiopathic pulmonary fibrosis," *Thorax,* vol. 68, pp. 1114-1121, 2013.

[6] S. Rahaman, L. Grove, S. Paruchuri, B. Southern, S. Abraham, K. Niese, R. Scheraga, S. Ghosh, C. Thodeti, D. Zhang, M. Moran, W. Schilling, D. Tschumperlin and M. Olman, "TRPV4 mediates myofibroblast differentiation and pulmonary fibrosis in mice," *J. Clin. Invest,* vol. 124, pp. 525-5238, 2014.

[7] M. Baxter, S. Eltom, B. Dekkak, L. Yew-Booth, E. Dubuis, S. Maher, M. Belvisi and M. Birrell, "Role of transient receptor potential and pannexin channels in cigarette smoke-triggered ATP release in the lung," *Thorax,* vol. 69, pp. 1080-1089, 2014.

[8] B. Nilius and V. Flockerzi, "Mammalian Transient Receptor Potential (TRP) Cation Channels," *Handbook of Experimental Pharmacology,* vol. 222, pp. 1-726, 2014.

[9] R. J. Thompson, "Pannexin channels and ischaemia," *J. Physiol.,* vol. 593, pp. 3463-3470, 2015.

[10] B. Isakson and R. Thompson, "Pannexin-1 as a potentiator of ligand-gated receptor signaling," *Channels (Austin.),* vol. 8, pp. 118-123, 2014.

[11] C. Giaume, L. Leybaert, C. Naus and J. Saez, "Connexin and pannexin hemichannels in brain glial cells: properties, pharmacology, and roles.," *Front. Pharmacol.,* vol. 4, pp. 88-95, 2013.

[12] J. Sandilos and D. Bayliss, "Physiological mechanisms for the modulation of pannexin 1 channel activity," *J. Physiol.,* vol. 590, pp. 6257-6266, 2012.

[13] H. Mihara, N. Suzuki, A. Boudaka, J. Muhammad, M. Tominaga, Y. Tabuchi and T. Sugiyama, "Transient receptor potential vanilloid 4-dependent calcium influx and ATP release in mouse and rat gastric epithelia," *World J.Gastroenterol.,* vol. 22, pp. 5512-5519, 2016.

[14] H. Mihara, A. Boudaka, T. Sugiyama, Y. Moriyama and M. Tominaga, "Transient receptor

AJRCMB Articles in Press. Published on 02-February-2018 as 10.1165/rcmb.2017-0413OC

potential vanilloid 4 (TRPV4)-dependent calcium influx and ATP release in mouse oesophageal keratinocytes," *J. Physiol.,* vol. 589, pp. 3471-3482, 2011.

[15] T. Miyamoto, T. Mochizuki, H. Nakagomi, S. Kira, M. Watanabe, Y. Takayama, Y. Suzuki, S. Koizumi, M. Takeda and M. Tominaga, "Functional role for Piezo1 in stretch-evoked Ca(2)(+) influx and ATP release in urothelial cell cultures," *J. Biol. Chem,* vol. 289, pp. 16565-16575, 2014.

[16] L. Janssen, L. Farkas, T. Rahman and M. Kolb, "ATP stimulates Ca(2+)-waves and gene expression in cultured human pulmonary fibroblasts.," *Int. J. Biochem. Cell Biol.,* vol. 41, pp. 2477-2484, 2009.

[17] M. Rahman, S. Mukherjee, W. Sheng, B. Nilius and L. Janssen, "Electrophysiological characterization of voltage-dependent calcium currents and TRPV4 currents in human pulmonary fibroblasts.," *Am. J. Physiol Lung Cell Mol. Physiol.,* vol. 310, pp. L603-L614, 2016.

[18] A. Garcias-Elias, S. Mrkonjic, C. Jung, C. Pardo-Pastor, R. Vicente and M. Valverde, "The TRPV4 Channel," *Handbook of Experimental Pharmacology,* vol. 222, pp. 293-319, 2014.

[19] B. Nilius, J. Vriens, J. Prenen, G. Droogmans and T. Voets, "TRPV4 calcium entry channel: a paradigm for gating diversity," *Am. J. Physiol Cell Physiol.,* vol. 286, pp. C195-C205, 2004.

[20] W. Everaerts, B. Nilius and G. Owsianik, "The vanilloid transient receptor potential channel TRPV4: from structure to disease," *Prog. Biophys. Mol. Biol.,* vol. 103, pp. 2-17, 2010.

[21] K. Thorneloe, A. Sulpizio, Z. Lin, D. Figueroa, A. Clouse, G. McCafferty, T. Chendrimada, E. Lashinger, E. Gordon, L. Evans, B. Misajet, D. Demarini, J. Nation, L. Casillas, R. Marquis, B. Votta, S. Sheardown, X. Xu and D. Brooks, "N-((1S)-1-{[4-((2S)-2-{[(2,4-dichlorophenyl)sulfonyl]amino}-3-hydroxypropanoyl)-1 -piperazinyl]carbonyl}-3-methylbutyl)-1-benzothiophene-2-carboxamide (GSK1016790A), a novel and potent transient receptor potential vanilloid 4 channel agonist induces urina," *J. Pharmacol. Exp. Ther.,* vol. 326, pp. 432-442, 2008.

[22] R. Alexander, A. Kerby, A. Aubdool, A. Power, S. Grover, C. Gentry and A. Grant, "4alpha-phorbol 12,13-didecanoate activates cultured mouse dorsal root ganglia neurons independently of TRPV4," *Br. J. Pharmacol.,* vol. 168, pp. 761-772, 2013.

[23] J. White, M. Cibelli, L. Urban, B. Nilius, J. McGeown and I. Nagy, "TRPV4: Molecular Conductor of a Diverse Orchestra," *Physiol. Rev.,* vol. 96, pp. 911-973, 2016.

[24] F. Vincent, A. Acevedo, M. Nguyen, M. Dourado, J. DeFalco, A. Gustafson, P. Spiro, D. Emerling, M. Kelly and M. Duncton, "Identification and characterization of novel TRPV4 modulators," *Biochem. Biophys. Res. Commun.,* vol. 389, pp. 490-494, 2009.

[25] A. Pinheiro, D. Paramos-de-Carvalho, M. Certal, C. Costa, M. Magalhaes-Cardoso, F. Ferreirinha, M. Costa and P. Correia-de-Sa, "Bradykinin-induced Ca2+ signaling in human subcutaneous fibroblasts involves ATP release via hemichannels leading to P2Y12 receptors activation," *Cell Commun. Signal.,* vol. 11, pp. 70-85, 2013.

[26] S. Penuela, R. Gehi and D. Laird, "The biochemistry and function of pannexin channels," *Biochim. Biophys. Acta,* vol. 1828, pp. 15-22, 2013.

[27] K. Schalper, M. Riquelme, M. Branes, A. Martinez, J. Vega, V. Berthoud, M. Bennett and J. Saez, "Modulation of gap junction channels and hemichannels by growth factors," *Mol.*

*Biosyst.,* vol. 8, pp. 685-698, 2012.

[28] W. Silverman, S. Locovei and G. Dahl, "Probenecid, a gout remedy, inhibits pannexin 1 channels," *Am. J. Physiol Cell Physiol,* vol. 295, pp. C761-C767, 2008.

[29] K. Engelhardt, M. Schmidt, M. Tenbusch and R. Dermietzel, "Effects on channel properties and induction of cell death induced by c-terminal truncations of pannexin1 depend on domain length.," *J. Membr. Biol.,* vol. 248, pp. 285-294, 2015.

[30] A. Boyd-Tressler, S. Penuela, D. Laird and G. Dubyak, "Chemotherapeutic drugs induce ATP release via caspase-gated pannexin-1 channels and a caspase/pannexin-1-independent mechanism," *J. Biol. Chem.,* vol. 289, pp. 27246-27263, 2014.

[31] F. Chekeni, M. Elliott, J. Sandilos, S. Walk, J. Kinchen, E. Lazarowski, A. Armstrong, S. Penuela, D. Laird, G. Salvesen, B. Isakson, D. Bayliss and K. Ravichandran, "Pannexin 1 channels mediate 'find-me' signal release and membrane permeability during apoptosis," *Nature,* vol. 467, pp. 863-867, 2010.

[32] R. Bruzzone, M. Barbe, N. Jakob and H. Monyer, "Pharmacological properties of homomeric and heteromeric pannexin hemichannels expressed in Xenopus oocytes.," *J. Neurochem.,* vol. 92, pp. 1033-1043, 2005.

[33] S. Mukherjee, F. Duan, M. Kolb and L. Janssen, "Platelet derived growth factor-evoked Ca(2+) wave and matrix gene expression through phospholipase C in human pulmonary fibroblast.," *Int.J.Biochem.Cell Biol.,* vol. 45, pp. 1516-1524, 2013.

[34] S. Mukherjee, E. Ayaub, J. Murphy, C. Lu, M. Kolb, K. Ask and L. Janssen, "Disruption of Calcium Signaling in Fibroblasts and Attenuation of Bleomycin-Induced Fibrosis by Nifedipine," *Am. J. Respir. Cell Mol. Biol.,* vol. 53, pp. 450-458, 2015.

[35] S. Mukherjee, M. Kolb, F. Duan and L. Janssen, "Transforming growth factor-beta evokes Ca2+ waves and enhances gene expression in human pulmonary fibroblasts," *Am. J. Respir. Cell Mol. Biol.,* vol. 46, pp. 757-764, 2012.

[36] M. Skals, R. Bjaelde, J. Reinholdt, K. Poulsen, B. Vad, D. Otzen, J. Leipziger and H. Praetorius, "Bacterial RTX toxins allow acute ATP release from human erythrocytes directly through the toxin pore," *J. Biol. Chem.,* vol. 289, pp. 19098-19109, 2014.

[37] P. Wong, R. Roberts and M. Randall, "Sex differences in the role of transient receptor potential (TRP) channels in endothelium-dependent vasorelaxation in porcine isolated coronary arteries.," *Eur. J. Pharmacol.,* vol. 750, pp. 108-117, 2015.

[38] B. Khakh, G. Burnstock, C. Kennedy, B. King, R. North, P. Seguela, M. Voigt and P. Humphrey, "International union of pharmacology. XXIV. Current status of the nomenclature and properties of P2X receptors and their subunits.," *Pharmacol. Rev.,* vol. 53, pp. 107-118, 2001.

[39] K. Tousova, L. Vyklicky, K. Susankova, J. Benedikt and V. Vlachova, "Gadolinium activates and sensitizes the vanilloid receptor TRPV1 through the external protonation sites.," *Mol. Cell Neurosci.,* vol. 30, pp. 207-217, 2005.

[40] L. Robson and M. Hunter, "Role of cell volume and protein kinase C in regulation of a Cl-conductance in single proximal tubule cells of Rana temporaria.," *J. Physiol.,* vol. 496, pp. 1-7, 1994.

[41] T. Tokimasa and R. North, "Effects of barium, lanthanum and gadolinium on endogenous chloride and potassium currents in Xenopus oocytes.," *J. Physiol.,* vol. 496, pp. 677-686,

AJRCMB Articles in Press. Published on 02-February-2018 as 10.1165/rcmb.2017-0413OC

1996.

[42] J. Zhang and M. Lieberman, "Chloride conductance is activated by membrane distention of cultured chick heart cells.," *Cardiovasc. Res.,* vol. 32, pp. 168-179, 1996.

[43] S. Pedersen, Y. Okada and B. Nilius, "Biophysics and Physiology of the Volume-Regulated Anion Channel (VRAC)/Volume-Sensitive Outwardly Rectifying Anion Channel (VSOR).," *Pflugers Arch.,* vol. 468, pp. 371-383, 2016.

[44] S. Pedersen, T. Klausen and B. Nilius, "The identification of a volume-regulated anion channel: an amazing Odyssey.," *Acta Physiol (Oxf),* vol. 213, pp. 868-881, 2015.

[45] S. Jung, A. Muhle, M. Schaefer, R. Strotmann, G. Schultz and T. Plant, "2003. Lanthanides potentiate TRPC5 currents by an action at extracellular sites close to the pore mouth.," *J.Biol.Chem.,* vol. 278, pp. 3562-3571, 2003.

[46] A. V. Zholos, "TRPC5.," *Handb.Exp.Pharmacol.,* vol. 222, pp. 129-156, 2014.

[47] D. Draganov, S. Gopalakrishna-Pillai, Y. Chen, N. Zuckerman, S. Moeller, C. Wang, D. Ann and P. Lee, "Modulation of P2X4/P2X7/Pannexin-1 sensitivity to extracellular ATP via Ivermectin induces a non-apoptotic and inflammatory form of cancer cell death.," *Sci. Rep.,* vol. 5, p. 16222, 2015.

[48] S. Bonvini, M. Birrell, M. Grace, S. Maher, J. Adcock, M. Wortley, E. Dubuis, Y. Ching, A. Ford, F. Shala, M. Miralpeix, G. Tarrason, J. Smith and M. Belvisi, "Transient receptor potential cation channel, subfamily V, member 4 and airway sensory afferent activation: Role of adenosine triphosphate.," *Journal of Allergy Clinical Immunology,* vol. 138, no. 1, pp. 249-26, 2016.

[49] Z. Ma, J. Tanis, A. Taruno and J. Foskett, "Calcium homeostasis modulator (CALHM) ion channels.," *Pflugers Arch.,* vol. 468, pp. 395-403, 2016.

[50] R. Bruzzone, S. Hormuzdi, M. Barbe, A. Herb and H. Monyer, "Pannexins, a family of gap junction proteins expressed in brain.," *Proc. Natl. Acad. Sci.U.S.A,* vol. 100, pp. 13644-13649, 2003.

## FIGURE LEGENDS

**Figure 1. Development of TRPV4-triggered membrane current**

HPFs were probed using ramp depolarizing commands at 15 second intervals before and during application of 4αPDD in the presence/absence of various pharmacological blockers, as indicated **(A)** Magnitudes of inward current obtained at -35 mV in individual cells during each ramp depolarizing command; all cells received 4αPDD (5 μM), but each had been pretreated with one or another blocker, as indicated. Inset shows the exact same data, but on a greatly expanded vertical axis). **(B)** Mean magnitudes (+/- SEM) of inward current measured at -80 mV at 5 minute intervals of all cells studied using the approach represented in (A). Symbols contained within boxes marked with asterisks are significantly different from the control values at that time point (ANOVA).

**Figure 2. Electrophysiological properties of 4αPDD– and ATP–evoked currents**

**(A)** I-V relationship of 4αPDD–evoked current in one representative cell in the presence/absence of CBX (100 μM) or apyrase (10 units), as indicated. **(B)** I-V relationship of ATP–evoked current in one representative cell in the presence or absence of $Gd^{3+}$ (1 mM), as indicated. **(C)** Magnitudes of ATP–evoked current recorded in one cell at -80 mV (bottom panel; determined at 20 second intervals using ramp depolarizing commands, as described in Figure 1A), as well as $V_{rev}$ for those currents (top panel). **(D)** $V_{rev}$ for 4αPDD–evoked currents in the presence or absence of various blockers, as indicated. Small diamonds indicate the most negative and most positive $V_{rev}$ (open and filled symbols, respectively) obtained in the various cells tested; large boxes indicate mean values of the same. A similar examination was also done for ATP–evoked current (far right).

AJRCMB Articles in Press. Published on 02-February-2018 as 10.1165/rcmb.2017-0413OC

**Figure 3: Time-course of 4αPDD–stimulated release of ATP.**

Mean determinations (3 separate runs of the assay; duplicate measurements made within each run) of ATP-content of supernatant overlying HPFs stimulated with 4αPDD (5 μM) using a luciferase assay (see Methods for details regarding sampling rate and data handling). To control for inter-assay variability (especially vis-à-vis cell density), and because luminescence was not detectable at time points less than 20 minutes, all data are standardized using the measurement obtained at 20 minutes within each run. Three other samples assayed at 30 minutes in the presence of apyrase (10 units) exhibited no accumulation of ATP (*, $p<0.05$ versus control at 30 minutes).

**Figure 4: Western blots for pannexin and TRPV4 proteins**

(A) Representative immunoblot image showing the presence of pannexin 1 and TRPV4 channels in normal HPFs from three different patients (relative to GAPDH). These blots are representative of two replicate determinations from three other patients. (B) PCR blot of samples from cells which were treated with siRNA directed against PANX1 (right) or with a scrambled control siRNA (middle), or which were not treated (left), showing specific elimination of PANX1 mRNA. (C) Mean 4αPDD-evoked currents at 5 minute intervals in cells which had been treated with PANX1 siRNA (filled circles; nine out of ten cells tested) or with control scrambled siRNA (open circles; seven cells tested), showing essentially complete elimination of the 4αPDD-evoked current. One of the ten cells pretreated with PANX1 siRNA still exhibited a substantial membrane current response to 4αPDD, albeit much smaller than those seen in the

control cells pretreated with scrambled siRNA construct, and was not included in the statistical analysis.

**Figure 5: 4α-PDD evokes calcium-flashes which are blocked by PPADS**

(A) Number of cells exhibiting a calcium-flash observed within any given video-frame in one complete video-recording having 8 active cells in the field of view (some other cells were visible, but exhibited no calcium-flash at all during the duration of this 70 minute recording; see Methods for details). The incidence of calcium-flashing was markedly increased by 4α-PDD (5 μM), and that in turn was nearly eliminated by subsequent addition of PPADS (10 μM). (B) Mean number (+/- SEM) of calcium-flashes observed during the 10 minute period immediately prior to addition of 4α-PDD (5 μM) in five different videorecordings, as well as the 10 minute period immediately afterward, as indicated; also shown is the mean number of calcium-flashes during the 10 minute period immediately after addition of PPADS (done in two of these five videorecordings).

**Figure 6: Overall model** Model of the mechanism which integrates our observations. The three different conductances which become activated following stimulation with 4α-PDD (indicated in the shaded boxes) and the physiological changes each produces are indicated, as well as the locus of action of the various blockers which we employed (italicized).

AJRCMB Articles in Press. Published on 02-February-2018 as 10.1165/rcmb.2017-0413OC

Figure 1

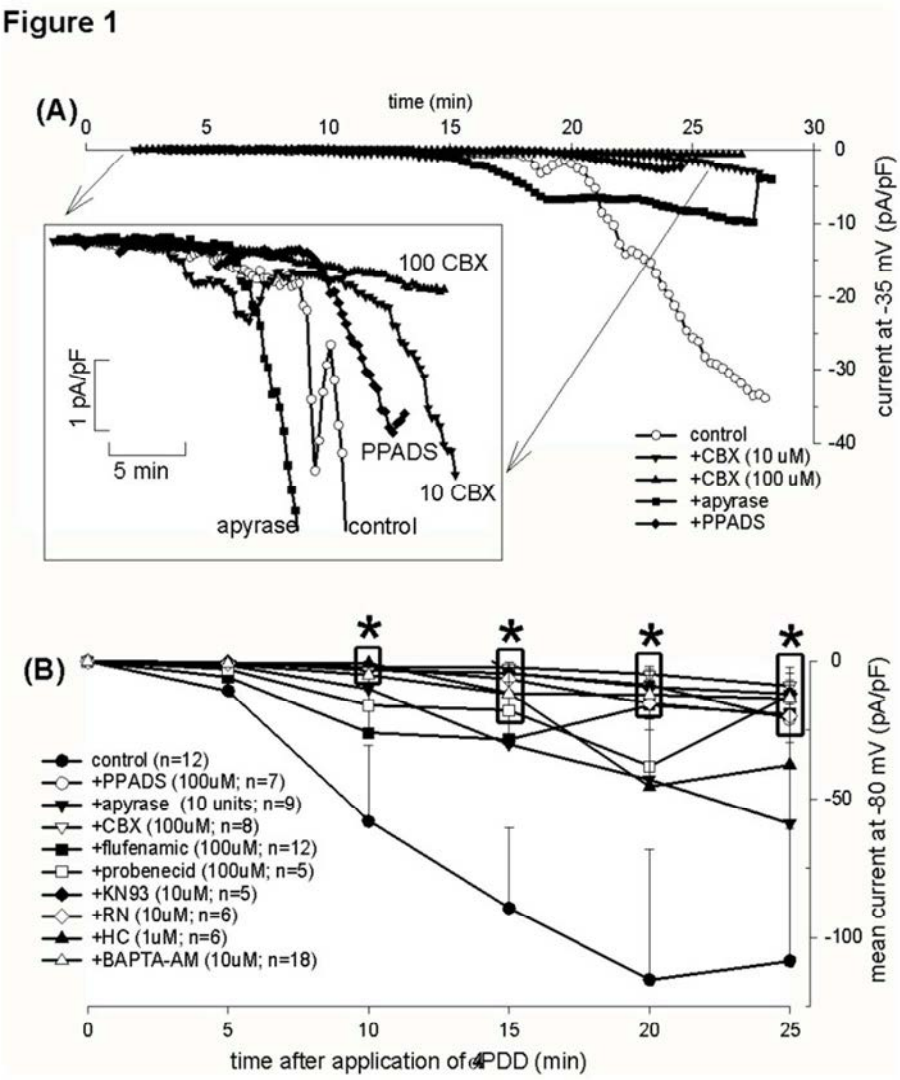


Figure 1. Development of TRPV4-triggered membrane current
HPFs were probed using ramp depolarizing commands at 15 second intervals before and during application of 4αPDD in the presence/absence of various pharmacological blockers, as indicated (A) Magnitudes of inward current obtained at -35 mV in individual cells during each ramp depolarizing command; all cells received 4αPDD (5 μM), but each had been pretreated with one or another blocker, as indicated. Inset shows the exact same data, but on a greatly expanded vertical axis). (B) Mean magnitudes (+/- SEM) of inward current measured at -80 mV at 5 minute intervals of all cells studied using the approach represented in (A). Symbols contained within boxes marked with asterisks are significantly different from the control values at that time point (ANOVA).

327x385mm (72 x 72 DPI)

AJRCMB Articles in Press. Published on 02-February-2018 as 10.1165/rcmb.2017-0413OC


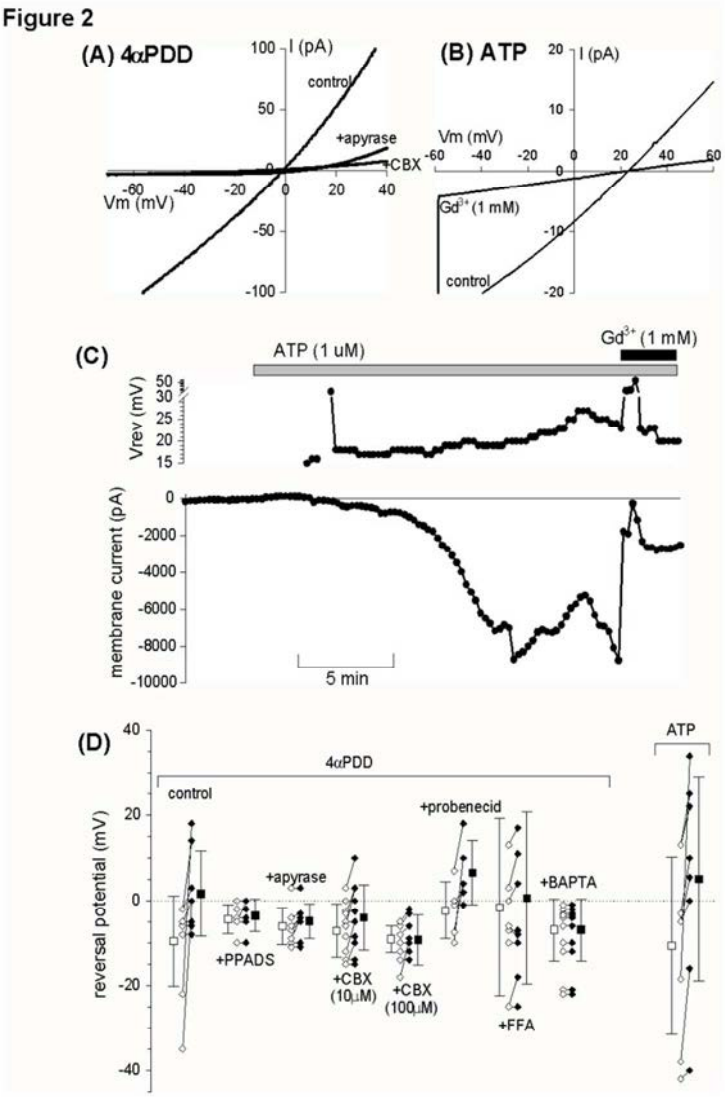


Figure 2. Electrophysiological properties of 4αPDD– and ATP–evoked currents
(A) I-V relationship of 4αPDD–evoked current in one representative cell in the presence/absence of CBX (100 μM) or apyrase (10 units), as indicated. (B) I-V relationship of ATP–evoked current in one representative cell in the presence or absence of Gd3+ (1 mM), as indicated. (C) Magnitudes of ATP–evoked current recorded in one cell at -80 mV (bottom panel; determined at 20 second intervals using ramp depolarizing commands, as described in Figure 1A), as well as Vrev for those currents (top panel). (D) Vrev for 4αPDD–evoked currents in the presence or absence of various blockers, as indicated. Small diamonds indicate the most negative and most positive Vrev (open and filled symbols, respectively) obtained in the various cells tested; large boxes indicate mean values of the same. A similar examination was also done for ATP–evoked current (far right).

336x488mm (72 x 72 DPI)

AJRCMB Articles in Press. Published on 02-February-2018 as 10.1165/rcmb.2017-0413OC

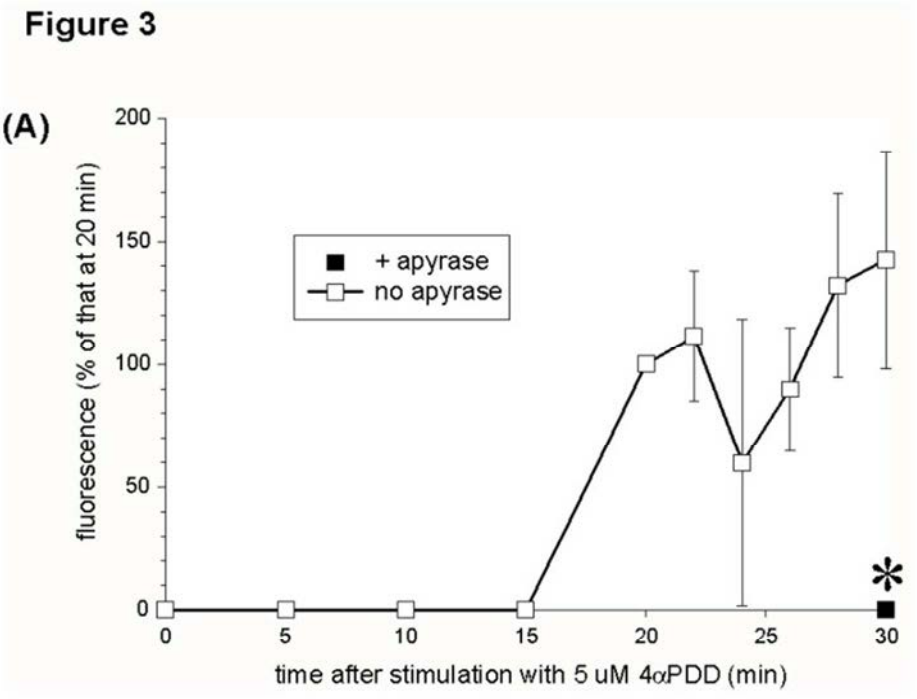


Figure 3: Time-course of 4αPDD–stimulated release of ATP.
Mean determinations (3 separate runs of the assay; duplicate measurements made within each run) of ATP-content of supernatant overlying HPFs stimulated with 4αPDD (5 μM) using a luciferase assay (see Methods for details regarding sampling rate and data handling). To control for inter-assay variability (especially vis-à-vis cell density), and because luminescence was not detectable at time points less than 20 minutes, all data are standardized using the measurement obtained at 20 minutes within each run. Three other samples assayed at 30 minutes in the presence of apyrase (10 units) exhibited no accumulation of ATP (*, $p<0.05$ versus control at 30 minutes).

291x226mm (72 x 72 DPI)

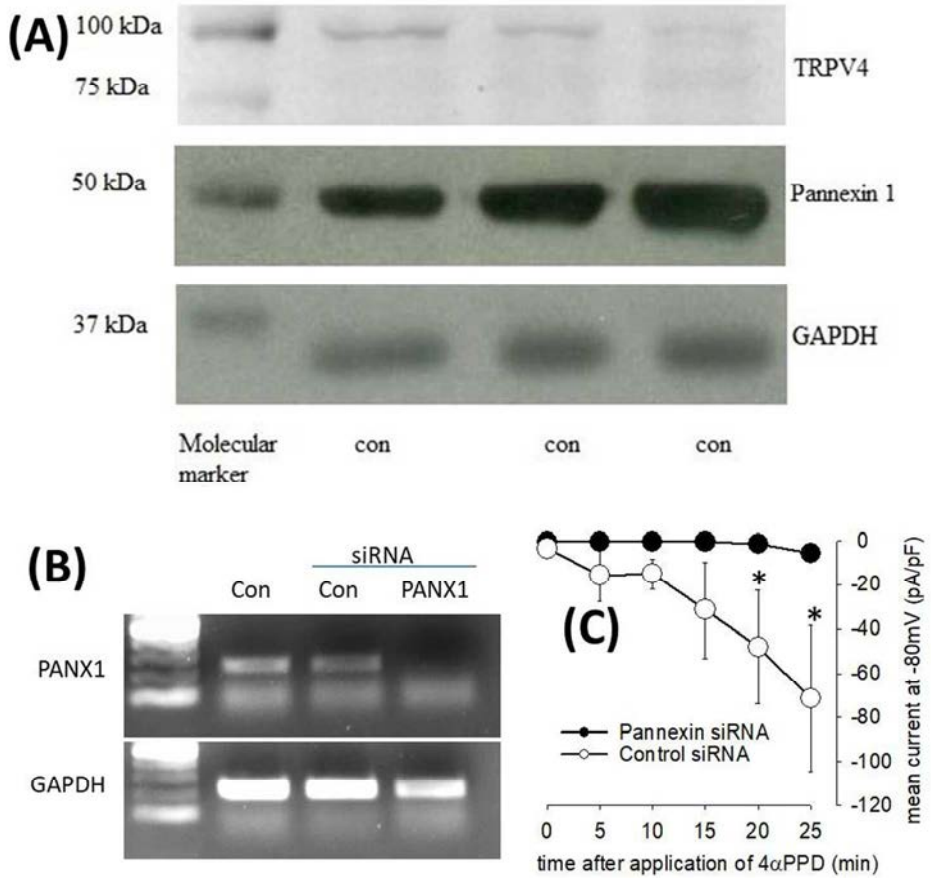


Figure 4: Western blots for pannexin and TRPV4 proteins
(A) Representative immunoblot image showing the presence of pannexin 1 and TRPV4 channels in normal HPFs from three different patients (relative to GAPDH). These blots are representative of two replicate determinations from three other patients. (B) PCR blot of samples from cells which were treated with siRNA directed against PANX1 (right) or with a scrambled control siRNA (middle), or which were not treated (left), showing specific elimination of PANX1 mRNA. (C) Mean 4αPDD-evoked currents at 5 minute intervals in cells which had been treated with PANX1 siRNA (filled circles; nine out of ten cells tested) or with control scrambled siRNA (open circles; seven cells tested), showing essentially complete elimination of the 4αPDD-evoked current. One of the ten cells pretreated with PANX1 siRNA still exhibited a substantial membrane current response to 4αPDD, albeit much smaller than those seen in the control cells pretreated with scrambled siRNA construct, and was not included in the statistical analysis.

164x146mm (150 x 150 DPI)

AJRCMB Articles in Press. Published on 02-February-2018 as 10.1165/rcmb.2017-0413OC

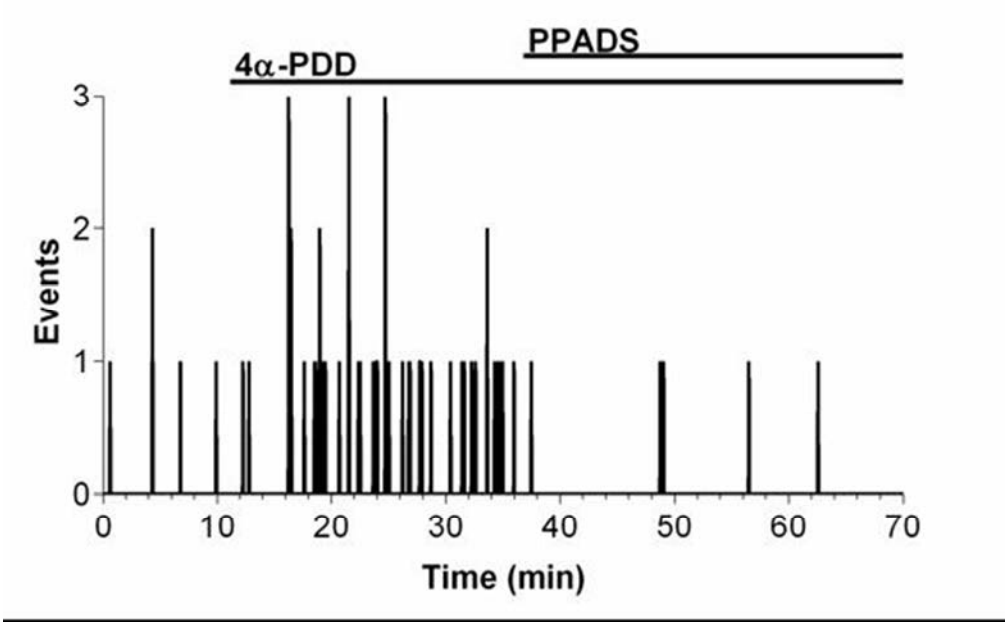


Figure 5: 4α-PDD evokes calcium-flashes which are blocked by PPADS
(A) Number of cells exhibiting a calcium-flash observed within any given video-frame in one complete video-recording having 8 active cells in the field of view (some other cells were visible, but exhibited no calcium-flash at all during the duration of this 70 minute recording; see Methods for details). The incidence of calcium-flashing was markedly increased by 4α-PDD (5 μM), and that in turn was nearly eliminated by subsequent addition of PPADS (10 μM).

150x93mm (96 x 96 DPI)

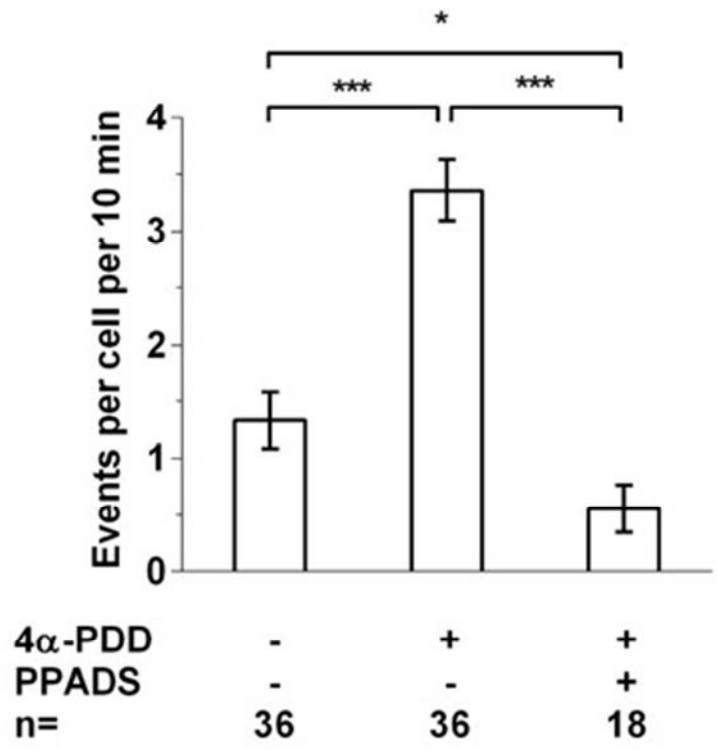


Figure 5: 4α-PDD evokes calcium-flashes which are blocked by PPADS
(B) Mean number (+/- SEM) of calcium-flashes observed during the 10 minute period immediately prior to addition of 4α-PDD (5 μM) in five different videorecordings, as well as the 10 minute period immediately afterward, as indicated; also shown is the mean number of calcium-flashes during the 10 minute period immediately after addition of PPADS (done in two of these five videorecordings).

98x105mm (96 x 96 DPI)

AJRCMB Articles in Press. Published on 02-February-2018 as 10.1165/rcmb.2017-0413OC

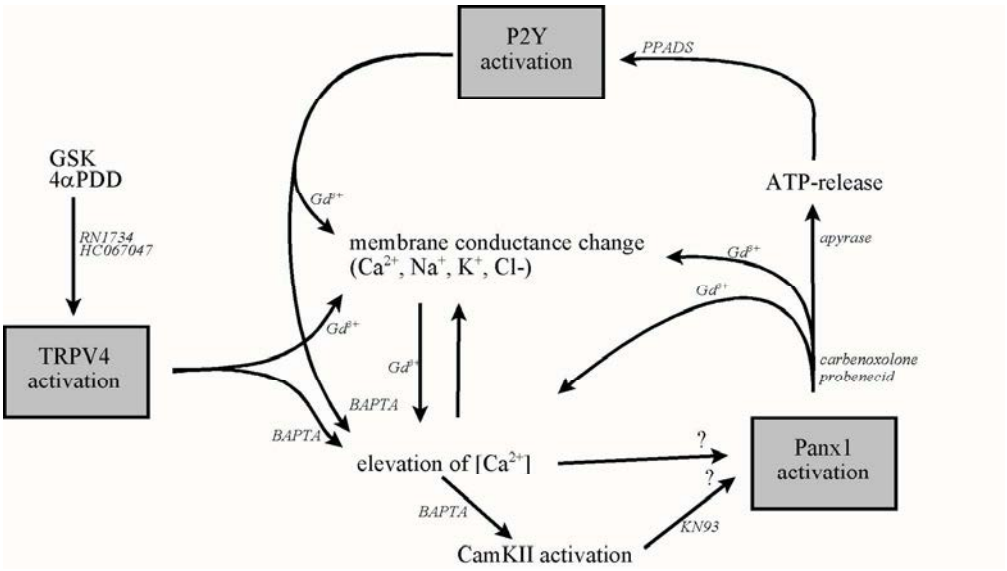


Figure 6: Overall model Model of the mechanism which integrates our observations. The three different conductances which become activated following stimulation with 4α-PDD (indicated in the shaded boxes) and the physiological changes each produces are indicated, as well as the locus of action of the various blockers which we employed (italicized).

704x396mm (72 x 72 DPI)

**ONLINE SUPPLEMENT**

## Isolation and Culture of Fibroblasts

All experimental procedures were approved by the St Joseph's Hospital Board of Ethics. HPFs were obtained from the lungs of six patients (three male and three female; aged 60–80 yr) undergoing lung surgery for pulmonary nodules following informed consent. None of the patients had major respiratory co-morbidities or lung function abnormalities. Normal lung tissues were taken from macroscopically-normal lung areas, as distant from the nodules as possible, and cultivated in 35 mm tissue culture dishes in explant medium (DMEM +20% FBS + antibiotics; filtered through 0.22μm filter) at $37^0$C in 95% air, 5% $CO_2$. After 2 to 3 weeks, cells were lifted by trypsin-EDTA treatment and sub-cultured in 75 $cm^2$ culture flask for further growth. These cells, designated passage 1, were cultivated in standard growth medium (RPMI + 10% FBS + antibiotics) at $37^0$C in 95% air, 5% $CO_2$ and the culture medium was changed three times a week. These were grown in Petri dishes till they became confluent, then were trypsin-lifted and passaged. All cells in the experiments described below were used between passages 4-10.

## Solutions and drugs

All chemicals were obtained from Sigma-Aldrich Chemical Company, (ON, Canada) except for: TGFβ1 (PeproTech Inc.; NJ, USA); Dulbecco's medium (Thermo Fisher Scientific (ON, Canada); RN1734 (Menai, UK); 4αPDD (Enzo Pharma, New York); RPMI Medium 1640, (Gibco); carbonexolone Tocris Bioscience (Bristol, UK); BAPTA-AM (Invitrogen, CA, USA); and Hank's Balanced Salt Solution (Thermo Fisher Scientific; ON, Canada). TGFβ1 was prepared in 4 mM HCl / 0.1% BSA. All other pharmacological agents were prepared as stock

AJRCMB Articles in Press. Published on 02-February-2018 as 10.1165/rcmb.2017-0413OC

solutions in 95% EtOH (RN1734), DMSO (4α-PDD; BAPTA-AM; flufenamic acid; HC067047; KN93; GSK 1067047); dilute NaOH (probenecid acid); or dd$H_2O$ (pyridoxalphosphate-6-azo[benzene-2',4'-disulphonic acid] tetrasodium salt, PPADS; $Gd^{3+}$; $La^{3+}$; carbenoxolone; apyrase; ATP), then diluted with HBSS to get the desired concentration in the recording chamber. The final bath concentration of EtOH or DMSO during electrophysiological recording was 0.1% or less.

**Patch-clamp electrophysiology**

The whole-cell patch-clamp technique was applied using fibroblasts which had been freshly trypsinized so that the cells were balled up (it was too difficult to patch onto flattened cells). Glass electrodes with tip resistance of 3–6 MΩ were filled with $Cs^+$-aspartate-containing electrode solution containing 50 μM β–escin.

To block $K^+$-currents and shift the Cl- equilibrium potential to -50 mV, we substituted KCl in the electrode solution with 120 mM $Cs^+$-aspartate plus 20 mM CsCl; pH was adjusted to 7.2 using CsOH.

Standard bath Ringer's solution contained (in mM): 130 NaCl, 5 KCl, 1 $CaCl_2$, 1 $MgCl_2$, 10 HEPES, 10 glucose, pH 7.4 with NaOH.

All patch-clamp experiments were performed at room temperature (22ºC).

Membrane currents were monitored u sing an Axopatch-1B current-voltage amplifier and stored in a computer for analysis using standard software (Clampex10.0 and Clampfit 10.0, Axon Instruments, USA). Access resistance was generally less than 20 MΩ (never more than 40 MΩ), and 70% prediction and correction were employed.

**Confocal calcium fluorimetry**

Confluent batches of cells cultured in glass-bottom Petri dishes were loaded with the $Ca^{2+}$-sensitive dye Oregon Green (5 μM) for 40 min at 37ºC, then perfused with HBSS solution for 15 min to allow for complete dye hydrolysis. These were then studied by confocal fluorimetric microscopy at 37ºC using a custom-built apparatus, as we have described previously [16] [17] [33] [34] [35] . Images were acquired at 3 second intervals before and during application of 4αPDD (10 μM; some also subsequently received PPADS), and the number of calcium-flashes per frame observed under the various pharmacological conditions were quantified (see Data Analysis).

**ATP-assay**

Cultured cells were trypsinized, re-suspended, and then plated in 96-well plates for 2 days; this allowed them sufficient time to re-adhere and become confluent. On the day of assay, these were challenged with 4αPDD (5 μM) for varying periods of time, after which the supernatant overlying these cells was aspirated and assayed for ATP-content using a commercially-available bioluminescent ATP assay (Sigma Aldrich) at room temperature. This assay is based upon an ATP-dependent hydrolysis of luciferin by luciferase; fluorescence signals were obtained using a Junior LB 9509 luminometer (Berthold Technology, Germany). Each individual treatment condition was performed in duplicate. In the first run of this assay, ATP-content was assessed at 2 minute intervals, beginning at 20 minutes after challenge with 4αPDD. Since there was already abundant ATP detected at the first time-point (20 minutes), we repeated the assay two more times, now also including three additional samplings at 5 minute intervals immediately following challenge with 4αPDD. Data are not reported as concentrations of ATP,

AJRCMB Articles in Press. Published on 02-February-2018 as 10.1165/rcmb.2017-0413OC

since the latter is entirely dependent upon the number of fibroblasts in each well (which varied between wells and batches) and the volume of the medium surrounding those cells; as such, the concentrations determined in the entire well would not reflect the concentrations experienced by the cells and their neighbors in the patch-clamp experiments. Data were standardized against the readings obtained in each run at 20 minutes following challenge with 4αPDD.

In a follow-up assay, we compared ATP-content at 0 and 20 minutes in control cells or those which had been treated with silencing-RNA against pannexin channels, as well as a scrambled si-RNA probe.

**Western blots**

Proteins were extracted from cells, using RIPA buffer, as per manufacturer's instruction. In brief, treated cells were incubated with 1x RIPA buffer on ice for 5 minutes. After brief sonication, supernatant was collected by centrifuging at 14000 g for 10 min, and the amount of protein estimated by the Bradford method. 25 µg protein was used for SDS-PAGE. Western blot analysis was done as described previously [16]. Antibodies raised against TRPV4 or against Panx1 were obtained from Abcam (Toronto, ON, Canada). The immuno-specificities of the anti-Panx1 antibody [36] and the anti-TRPV4 antibody [37] have been verified elsewhere. The protein bands were detected using horseradish peroxidase-conjugated secondary antibody (1:2000 dilution) (Cell Signaling Technology, Whitby, ON, Canada) and Western blot detection reagent (GE Healthcare, Canada). The bands were digitized, subjected to densitometric scanning using a standard image program, and normalized against the loading control, GAPDH (Cell Signaling Technology).

**siRNA transfection**

Control siRNA was purchased from Qiagen, pannexin 1 siRNA (PANX1 siRNA) was purchased from Thermo Fisher Scientific. Silencing of PANX1 gene was done using Xfect siRNA transfection reagent (Clontech Laboratories Inc. CA, USA) according to manufacturer's instructions. Cells were cultured in a six-well plate until they were 90% confluent. Next, 30 pmol (3µl) siRNAs were diluted in 47 µl Xfect reaction buffer and mixed with 50 µl Xfect transfection polymer (4 µl Xfect Transfection polymer and 46 µl Xfect reaction buffer) to form transfection complex for 20 min at room temperature. These transfection complexes were then added to the cell culture media and the cells were incubated at 37°C in a $CO_2$ incubator for further 24-48 hr.

**RNA isolation and RT-PCR**

Total RNA was isolated as described previously [29], 1µg of RNA was treated with DNAse and reverse transcribed using qScript™ cDNA SuperMix (Quanta Bioscience, Gaithersburg, MD, USA). The cDNA was amplified by PCR, using Platinum PCR super mix (Invitrogen, Canada) following a semi-quantitative RT-PCR technique. PANX1and GAPDH primers used are listed below.

| | |
|---|---|
| PANX1 forward | 5'- TTTTCCCCTACATCCTGCTG – 3' |
| PANX1 reverse | 5'- CTCCCACAAACTTTGCCCTA - 3' |
| GAPDH forward | 5'- AGGGCTGCTTTTAACTCTGGT -3' |
| GAPDH reverse | 5'- CCCCACTTGATTTTGGAGGGA -3' |

The PCR products were visualized by electrophoresis in 1% agarose gel (Bio-Rad, CA, USA) with RedSafe Nucleic Acid staining solution (FroggaBio Inc, Toronto, Canada).